

## Dispersion relations for the $S$ , $P$ , $D$ and $F$ $\pi\pi$ amplitudes. Precise determination of the $f_0(500)$ and $f_0(980)$ parameters via dispersive analysis of the $\pi\pi$ data

**Robert Kamiński\***

*The Henryk Niewodniczański Institute of Nuclear Physics, Polish Academy of Sciences, Division of Theoretical Physics, 31-342 Kraków, Poland*

Recently new - one subtracted dispersion relations with imposed crossing symmetry condition for the  $\pi\pi$   $S, P, D$  - and  $F$ -wave scattering amplitudes have been derived and presented [1,2]. Together with the well known Roy equations with two subtractions they have led to unitary parameterization of many partial wave amplitudes in very wide energy range. They have allowed e.g. for a very precise, unambiguous and long waited determination of scattering lengths and parameters of the  $f_0(500)$  (often called  $\sigma$ ) and  $f_0(980)$  resonances in the  $S$  wave.

In this paper, general mathematical structure of these dispersion relations is presented. It is shown that these equations are very demanding i.e. produce output amplitudes with very small errors what significantly increases the accuracy of determined amplitudes.

The  $S$  and  $P$ -wave amplitudes have been directly fitted to the once subtracted dispersion relations (called GKPY - see [1]), forward dispersion relations, sum rules and experimental data including very recent  $K_{l4}$  one. Making analytic continuation of these two amplitudes to the complex energy plane, the parameters of the lowest resonances have been very precisely determined. For example the pole of  $f_0(600)$  has been found at  $(457^{+14}_{-13} - i279^{+11}_{-7})$  MeV and pole of  $f_0(980)$  at  $(996 \pm 7 - i25^{+10}_{-6})$  MeV. This led to significant changes in section of Particle Data Tables 2012 devoted for light scalar mesons in comparison with previous editions.

For all waves, the threshold parameters (scattering lengths and slopes) have been also very precisely determined.

It is worthy noting that although the presented here amplitudes of the  $D$  and  $F$  waves were not fitted directly to dispersion relations in [1], they fulfill crossing symmetry quite well up to  $\sim 800$  MeV (some work is still needed).

Those new, once subtracted dispersion relations for the  $\pi\pi$   $S, P, D$  - and  $F$  partial waves, form a complementary set of theoretical constraints that imposed on the amplitudes fitted only to experimental data can define them clearly and precisely. Example of practical application of the GKPY equation in the testing of such input amplitudes is presented and commented.

*The Xth conference Quark Confinement and the Hadron Spectrum, October 8-12, 2012, TUM Campus Garching Munich, Germany*

\*e-mail: [robert.kaminski@ifj.edu.pl](mailto:robert.kaminski@ifj.edu.pl)

## 1. Introduction

Recent dispersive analysis of  $\pi\pi$  scattering data (including very recent,  $K_{I4}$  experimental results) led to construction of the  $\pi\pi$  amplitudes in many partial waves ( $S, P, D$  and  $F$ ) [1, 2] and in energy range from the threshold to 1420 MeV. Higher energy isospin amplitudes were given by Regge parameterizations.

The real parts of these amplitudes (called input amplitudes) have been confronted with the output ones given by dispersive relations. The output amplitudes have been constructed after imposing the theoretical constraints from Roy-type dispersion relations, forward ones (FDR) and the sum rules for the threshold parameters (SR) [1], on the initial unconstrained fit to the data. All output amplitudes have been achieved with very high precision due to implementation of very demanding the Roy-type once subtracted dispersion relations with imposed crossing symmetry condition (for the  $S$  and  $P$  waves called GKPY equations, derived and presented in [1]).

The fact that, due to the very good fits, the  $S$  and  $P$  amplitudes fulfill conditions imposed by the dispersion relations (e.g. crossing symmetry), ensured that analytical continuation of these amplitudes on the complex energy plane provides reliable and precise information on the resonances e.g. the  $f_0(500)$  and  $f_0(980)$  in the  $S$  wave.

The GKPY dispersive equations relate imaginary part of the input ( $IN$ ) with real part of the output ( $OUT$ ) amplitudes  $t_\ell^I(s = m_\pi^2)$  and read

$$\text{Re } t_\ell^{I(OUT)}(s) = \sum_{I'=0}^2 C_{st}^{II'} a_0^{I'} + \sum_{I'=0}^2 \sum_{\ell'=0}^4 \int_{4m_\pi^2}^{\infty} ds' K_{\ell\ell'}^{II'}(s, s') \text{Im } t_{\ell'}^{I'(IN)}(s') \quad (1.1)$$

where  $a_0^{I'}$  are subtraction terms  $ST_\ell^I$  being combinations of the  $S$  wave scattering lengths given by threshold expansion  $\text{Re } t_\ell^I(p) = p^{2\ell}(a_\ell^I + p^2 b_\ell^I + \dots)$  and  $K_{\ell\ell'}^{II'}(s, s')$  are kernels derived by imposing  $s \leftrightarrow t$  crossing symmetry conditions on the  $\pi\pi \leftrightarrow \pi\pi$  amplitudes. Amplitudes  $t_\ell^I(s)$  are functions of experimentally determined phase shifts  $\delta_\ell^I(s)$  and inelasticities  $\eta_\ell^I(s)$

$$t_\ell^I(s) = \frac{\sqrt{s} \eta_\ell^I(s) e^{i\delta_\ell^I(s)} - 1}{2i\sqrt{s - 4m_\pi^2}}. \quad (1.2)$$

Integration region in Eq. (1.1) has been divided into two parts: for the kernel terms  $KT_\ell^I(s)$  and for driving ones  $DT_\ell^I(s)$  (presented in [1, 2]). The kernel terms account for contributions of all partial waves ( $\ell = 0 \dots 3$ ) at effective two pion mass smaller then  $\sqrt{s'_{max}} = 1.42$  GeV. The driving terms enclose contributions from the higher  $\sqrt{s'}$  region. The value of  $\sqrt{s'_{max}}$  is given by two pion mass up to which experimental data are sufficiently precise to determine the amplitudes  $t_\ell^I(s)$ .

## 2. Method and results

The fits have been controlled by difference  $\Delta(s_j) = | \text{Re } t_\ell^{I(OUT)}(s_j) - \text{Re } t_\ell^{I(IN)}(s_j) |$  which can be treated as measurement of fulfilment of crossing symmetry by analyzed amplitudes. The smaller this difference the better crossing symmetry for given amplitude is satisfied. Consistency check of the fit with all theoretical constraints has been done by minimization of the sum

$$\chi_{tot}^2 = \chi_{data}^2 + \bar{d}_{Roy}^2 + \bar{d}_{GKPY}^2 + \bar{d}_{FDR}^2 + \bar{d}_{SR}^2 \quad (2.1)$$

where  $\bar{d}_i^2 = \frac{1}{np} \sum_j^{np} \left( \frac{\Delta_i(s_j)}{\delta\Delta_i(s_j)} \right)^2$  are averaged distances of  $\Delta_i(s_j)$  taken with uncertainties  $\delta\Delta_i(s_j)$  calculated using Monte Carlo method (for details see [1, 2]).

In the initial fit, values of these averaged differences for the Roy and GKPY equations and for the FDR were:  $\bar{d}_{Roy}^2 = 0.87$ ,  $\bar{d}_{GKPY}^2 = 1.9$  and  $\bar{d}_{FDR}^2 = 2.0$  while corresponding values in the final fit were 0.14, 0.32, 0.4. Significant difference between averaged distance for the Roy equations and that for the GKPY is caused by much smaller values of  $\delta\Delta_i(s_j)$  above about 400 MeV in the GKPY equations than in the Roy ones.

The curves on Figures 1-6 present the input and output amplitudes for the GKPY equations and components  $ST_\ell^I, KT_\ell^I(s)$  and  $DT_\ell^I(s)$  of the output amplitudes for the  $S, P, D$  and  $F$ -waves. For the  $S$  and  $P$  waves the differences  $\Delta_i(s_j)$  are everywhere smaller than  $\delta\Delta_i(s_j)$ . Although the amplitudes of the  $D$  and  $F$  waves have not been fitted directly to dispersion relations and data as the  $S$  and  $P$  waves, they also indicate on quite good agreement between input and output amplitudes below  $\sim 800$  MeV. As was already noticed here and analysed in [1], very important advantage of the GKPY equations over the Roy ones is very slow increase of the output uncertainties. It is caused by fact that contrary to the Roy equations, the subtracting terms in the GKPY ones are constant and their errors do not propagate with increasing energy.

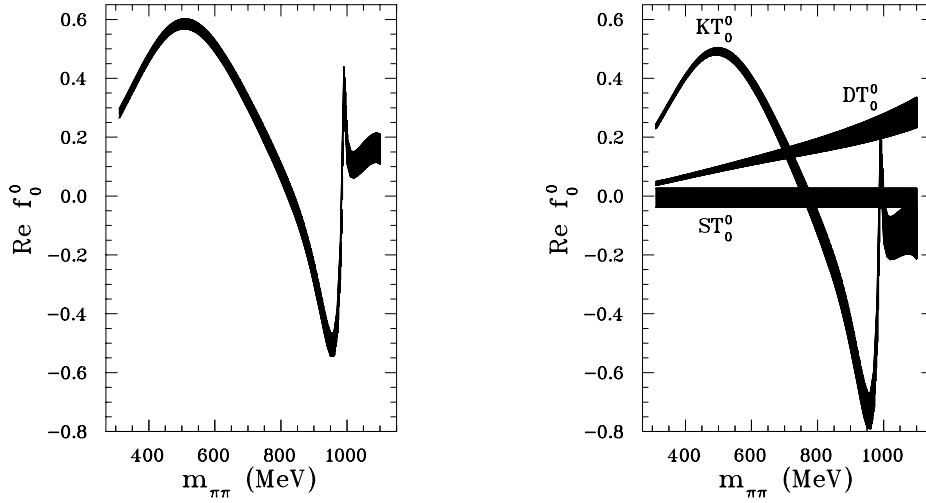


**Figure 1:** Left figure:  $\pi\pi$  input (solid line) and output (dashed line) amplitudes for the  $S_0$  wave together with output error band. Right figure: components of the  $S_0$  output amplitude - subtracting term (ST), kernel term (KT) and driving term (DT) together with corresponding error bands.

Existence of resonances is always associated with occurrence of poles at  $\sqrt{s_{pole}}$  in the complex energy plane. Relation between position of a given pole and parameters of a corresponding resonance can be expressed by  $M_{res} = Re(\sqrt{s_{pole}})$  and  $\Gamma_{res} = -2Im(s_{pole})$ . Making analytical continuation of the output amplitudes from the Roy and GKPY equations to the complex energy plane the poles related with resonances  $f_0(500)$ ,  $f_0(980)$  and  $\rho(770)$  have been found [3].

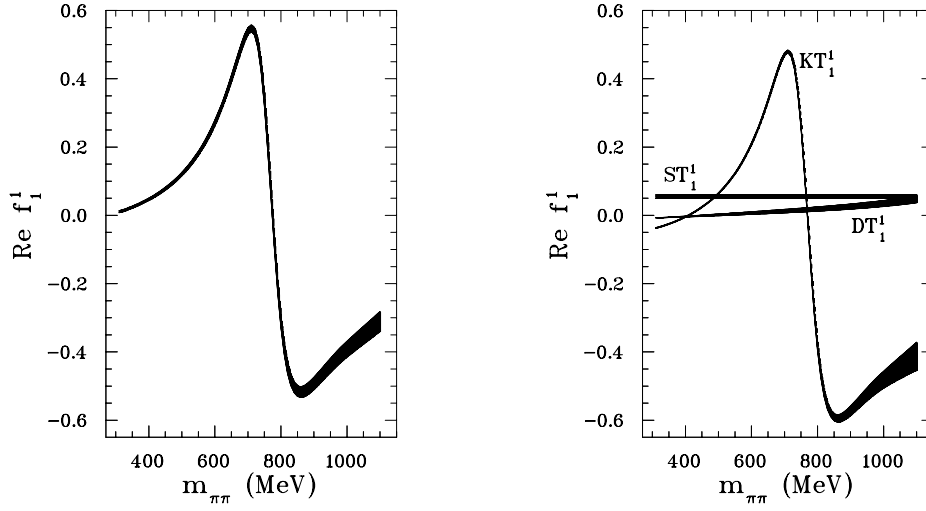


**Figure 2:** Left figure:  $\pi\pi$  input (solid line) and output (dashed line) amplitudes for the  $P1$  wave together with output error band. Right figure: components of the  $P1$  output amplitude - subtracting term (ST), kernel term (KT) and driving term (DT) together with corresponding error bands.

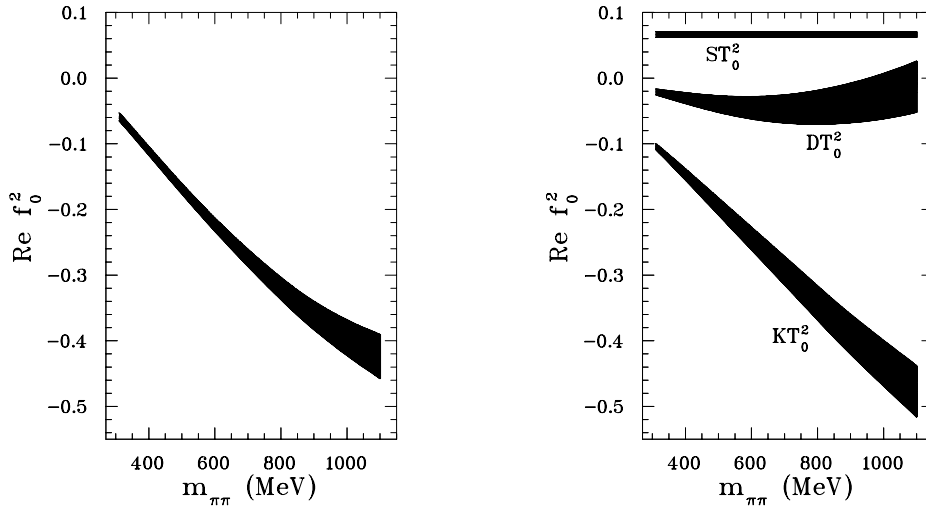


**Figure 3:** Left figure:  $\pi\pi$  input (solid line) and output (dashed line) amplitudes for the  $S2$  wave together with output error band. Right figure: components of the  $S2$  output amplitude - subtracting term (ST), kernel term (KT) and driving term (DT) together with corresponding error bands.

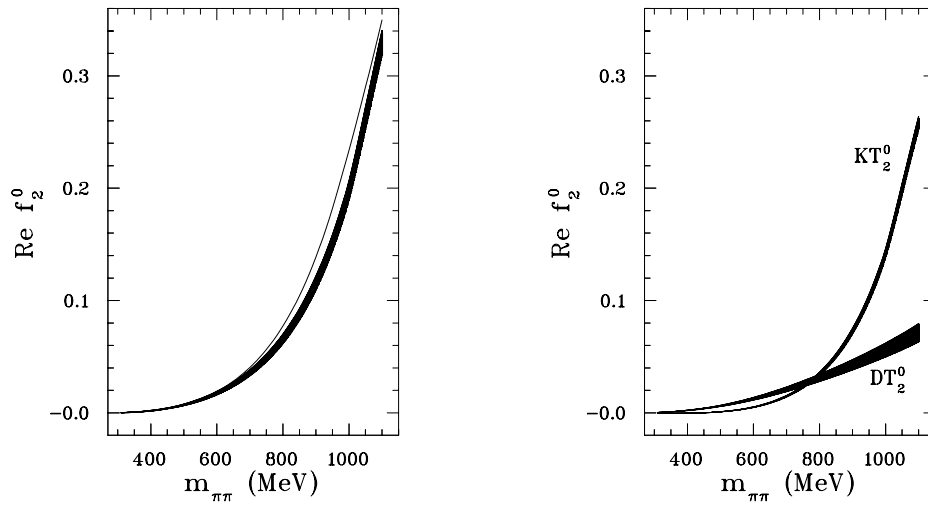


**Figure 4:** Left figure:  $\pi\pi$  input (solid line) and output (dashed line) amplitudes for the  $D_0$  wave together with output error band. Right figure: components of the  $D_0$  output amplitude - kernel term (KT) and driving term (DT) together with corresponding error bands.

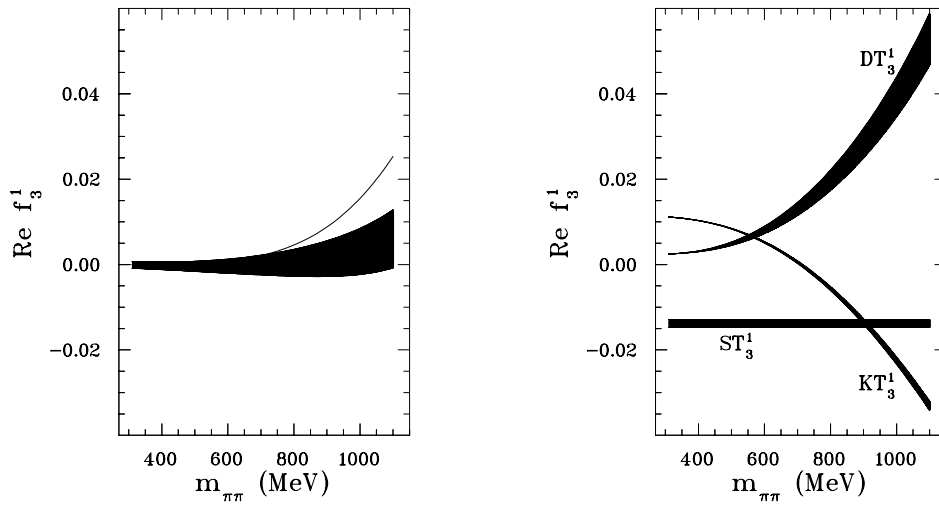


**Figure 5:** Left figure:  $\pi\pi$  input (solid line) and output (dashed line) amplitudes for the  $F_1$  wave together with output error band. Right figure: components of the  $F_1$  output amplitude - subtracting term (ST), kernel term (KT) and driving term (DT) together with corresponding error bands.

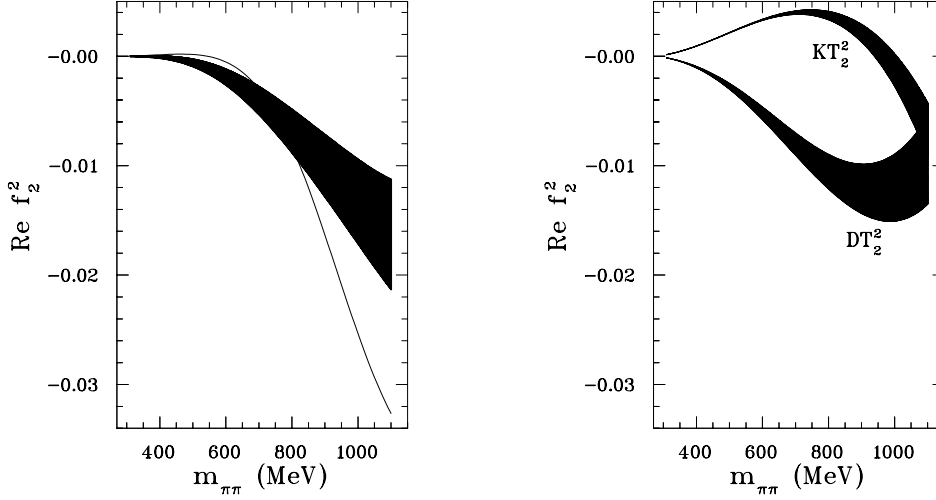


**Figure 6:** Left figure:  $\pi\pi$  input (solid line) and output (dashed line) amplitudes for the  $D_2$  wave together with output error band. Right figure: components of the  $D_2$  output amplitude - kernel term (KT) and driving term (DT) together with corresponding error bands.

	$\sqrt{s_{\text{pole}}} \text{ (MeV)}$	$ g $
$f_0(500)^{\text{GKPY}}$	$(457^{+14}_{-13}) - i(279^{+11}_{-7})$	$3.59^{+0.11}_{-0.13} \text{ GeV}$
$f_0(500)^{\text{Roy}}$	$(445 \pm 25) - i(278^{+22}_{-18})$	$3.4 \pm 0.5 \text{ GeV}$
$f_0(980)^{\text{GKPY}}$	$(996 \pm 7) - i(25^{+10}_{-6})$	$2.3 \pm 0.2 \text{ GeV}$
$f_0(980)^{\text{Roy}}$	$(1003^{+5}_{-27}) - i(21^{+10}_{-8})$	$2.5^{+0.2}_{-0.6} \text{ GeV}$
$\rho(770)^{\text{GKPY}}$	$(763.7^{+1.7}_{-1.5}) - i(73.2^{+1.0}_{-1.1})$	$6.01^{+0.04}_{-0.07}$
$\rho(770)^{\text{Roy}}$	$(761^{+4}_{-3}) - i(71.7^{+1.9}_{-2.3})$	$5.95^{+0.12}_{-0.08}$

**Table 1:** Poles and residues from Roy and GKPY equations

Apart of determination of those parameters, the analytical continuation of amplitudes allowed also to calculate couplings of resonances to the  $\pi\pi$  channel. The parameters of these poles and the couplings are presented in Table 1. The couplings are given by residues of the poles:

$$g^2 = -16\pi \lim_{s \rightarrow s_{\text{pole}}} (s - s_{\text{pole}}) t_\ell(s) (2\ell + 1) / (2p)^{2\ell} \quad (2.2)$$

where  $p^2 = s/4 - m_\pi^2$ . Analyzing results in Table 1 one can notice that central values of parameters of resonances and couplings for the Roy and GKPY equations differ only slightly and all are within the estimated errors. It confirms compatibility of the twice and once subtracted dispersion relations used in the fits. The only sizable difference is in the errors of positions of poles and couplings. Again, as it was for the values of averaged distances in the  $\chi^2$ , it is caused by much smaller uncertainties of the GKPY equations than those of the Roy equations.

Fig. 7 presents positions of the  $f_0(500)$  poles taken from Particle Data Group Tables (PDGT) 2010 [4] and of the  $f_0(500)$  pole found in presented analysis [3]. Also ranges of the mass and the width estimated in PDGT 2010 and 2012 [5] for the  $f_0(500)$  are shown for comparison. Striking feature of this comparison is significant difference between parameters estimated in the new tables and those in the previous ones. The mass of the  $f_0(500)$  has changed from  $M = 400 - 1200$  MeV to  $400 - 550$  MeV and the width from  $\Gamma = 500 - 1000$  MeV to  $400 - 700$  MeV.

Comparing estimations in those Particle Data Tables one can easily notice that apart of the changes in the central values of the parameters, very significant changes are in the accuracy of presented estimations. This is due to the recent dispersive analyzes of the  $\pi\pi$  amplitudes which incorporate either Roy or GKPY equations together with other theoretical constraints [1, 6]. In the presented here analysis the greatest impact on reduction of the errors had GKPY equations.

The estimated values of parameters for the next light scalar-isoscalar  $f_0(980)$  in PDGT 2012 are:  $M_{f_0(980)} = 990 \pm 20$  MeV and  $\Gamma_{f_0(980)} = 40 - 100$  MeV. The position of the pole found in presented here analysis completely agrees with this estimation and can be found in Table 1.

### 3. Application of the GKPY in modification of existing amplitudes

Very interesting example of practical application of the method described above is modification of the  $\pi\pi$  amplitudes not fulfilling the crossing symmetry conditions [7]. The initial amplitudes constructed by fits only to experimental data in the range from the  $\pi\pi$  threshold to about 1800 MeV [8], have been modified by adding the GKPY equations for the  $S$  and  $P$  waves. In results these amplitudes below about 1000 MeV have change dramatically. For example the  $f_0(500)$  pole at  $616.5 - i554.0$  MeV in the initial amplitude moved to  $473.7 - i297.8$  MeV in the final one i.e. to the position located about one standard deviation from the presented here. The threshold region below  $m_{\pi\pi} \approx 600$  MeV, excluded from analysis in the initial fit, has been very well described in the final fit and the threshold parameters achieved the same values as found in [1]. Important is to mention here that general mathematical structure of the parametrized initial amplitudes was not changed after modifications of the model while the total  $\chi^2$  decreased from almost 2.4 to 1.3.

### 4. Conclusions

In this short letter the basic points of new dispersive analysis of the  $\pi\pi$  amplitudes have been presented. The proposed here method of simultaneous analysis of theoretical constraints expressed by set of dispersion relations and experimental data is very efficient, precise and easy to use. Example of the importance of presented here dispersive analysis and its results can be seen in the new edition of the particle data tables [5] where parameters of the two lightest scalar-isoscalar mesons  $f_0(500)$  and  $f_0(980)$  have been changed (in the case of the  $f_0(500)$  - very significantly). Worthy is to note that even the name of the  $f_0(500)$  has been changed (previously was  $f_0(600)$ ).

One has to note also that, as was already discussed in [1, 3], the presented here results agree very well with those obtained by another, independent, group also using dispersive analysis and working on scalar meson spectroscopy for many years [6].

In this letter the example of practical implementation of the GKPY equations in modification of the  $\pi\pi$  amplitudes fitted only to experimental data has been shortly presented.

One can hope that proposed and presented here method will be widely used in various analyzes to determine or to correct  $\pi\pi$  amplitudes in many partial waves and in wide  $m_{\pi\pi}$  range.

## Acknowledgements

This work has been partly supported by the Polish Ministry of Science and Higher Education (grant No N N202 236940).

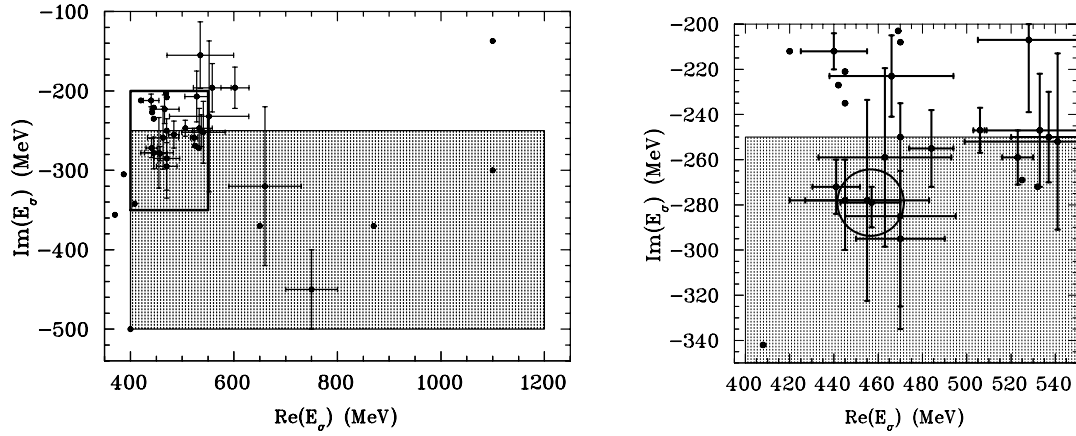


**Figure 7:** Positions of the poles (black dots) related with the  $f_0(500)$  (or  $\sigma$ ) cited in PDG'2010 [4], energy  $E_\sigma = \sqrt{s_\sigma}$ . Gray bands represent errors of mass and half of the width of the  $f_0(500)$  in PDG'2010. The rectangle on the left figure indicates the magnified area shown on the right drawing and corresponds to the errors of mass and half of the width of the  $f_0(500)$  in PDG'2012 [5]. The pole calculated in presented work lies in the middle of the circle.

## References

- [1] R. Garcia-Martin, R. Kamiński, J. Ruiz de Elvira, J. Pelaez and F. Yndurain, Phys. Rev. D **83**, 074004 (2011).
- [2] R. Kamiński, Phys. Rev. D **83**, 076008 (2011).
- [3] R. Garcia-Martin, R. Kamiński, J. Pelaez, J. Ruiz de Elvira, Phys. Rev. Lett. **107** (2011) 072001.
- [4] K. Nakamura et al. (Particle Data Group), J. Phys. **G37**, (2010) 075021
- [5] J. Beringer et al. (Particle Data Group), Phys. Rev. **D86**, (2012) 010001
- [6] I. Caprini, G. Colangelo, H. Leutwyler, Phys. Rev. Lett. **96**, (2006) 132001
- [7] P. Bydzovsky and R. Kamiński, Few-Body Syst, 2013, DOI 10.1007/s00601-012-0530-z.
- [8] Surovtsev et al., Phys. Rev. **D81**, (2010) 016001 **D85**, (2012) 036002